11. A. A. Borisov, B. E. Gel'fand, et al., "Amplification of shock waves in a liquid containing vapor bubbles," in: Nonlinear Wave Processes in Two-Phase Media [in Russian], ITF Sib. Otd. Akad. Nauk SSSR, Novosibirsk (1977).

STRONG ACTION OF A STRONGLY UNDEREXPANDED LOW-DENSITY JET ON A PLANE OBSTACLE

É. N. Voznesenskii and V. I. Nemchenko

UDC 532.525.6.011.5

One of the fundamental characteristics of the strong action of a freely expanding gas jet or a strongly underexpanded gas jet on an obstacle is the pressure distribution on the surface. For a phenomenological description of the interaction and development of engineering computation methods, it is also useful to know the shape of the shock which occurs here. Investigation of the interaction between a strongly underexpanded gas jet and a plane obstacle parallel to the jet axis should be extracted as a separate problem. All the results published in the literature [1-5] for the analysis of this problem have substantially been obtained in dense jets. Examples of specific pressure distributions on an obstacle are presented in [1-3], and in addition, methods are given for an approximate computation of the magnitude of the induced pressure. As a rule, different modifications of the Newton method or the method of tangential wedges are recommended. According to estimates [2, 4], the accuracy of such computations is not more than satisfactory and drops rapidly downstream. A search for other means of solving the problem, particularly for modeling the phenomena in wind tunnels with subsequent representation of the results in criterial form, is of interest. Such an approach is used in [4, 5], where similarity criteria are constructed for the dimensionless representation of the shock and the extension of the pressure distribution to a plate parallel to the jet axis on the basis of similarity theory and the criterial characteristics of a strongly underexpanded jet derived in [6], and appropriate empirical dependences are proposed for dense jets.

Data of an experimental investigation of an analogous problem, performed on low-density jets, are presented below.

The conditions characterizing the jet outflow (air is the working gas) are the following: stagnation pressure $p_0 = 4.13 \cdot 10^4$-$6.67 \cdot 10^4$ Pa, stagnation temperature $T_0 = 395$-780°K, pressure in the working chamber $p_\infty = 1.33$-13.3 Pa, degree of flow expansion $N = p_0/p_\infty = 0.5 \cdot 10^4$-$4 \cdot 10^4$ for nozzle Mach numbers determined without taking account of the boundary layer, $M_a = 1.0$-3.92. The distance $h = H/r_a$ between the model surface and the jet axis, expressed in nozzle exit section radii r_a varied between 4-20. Under conditions of the experiment $Re_L = Re_*/N^{1/2}$, where Re_* is the Reynolds number computed with respect to the critical gas parameters and the diameter of the nozzle critical section, varied between 14 and 160, i.e., was substantially less than the value $Re_L \sim 10^3$-10^4 characteristic for [1-5]. Therefore, according to the classification of the flow structure in a jet by the Reynolds numbers Re_L [7, 8], the investigation represented occupies a domain between the domain of interaction with a diffuse jet surface on the one hand, and a jet with a turbulent mixing layer on the other, and corresponds to the case of interaction of a completely laminar jet with an obstacle when the effects of viscosity and rarefaction still do not reach that part of the jet core in every case, by which the strong load on the obstacle is defined for the range of values of h presented.

Included in the paper are data of just those experiments in which the influence of a hanging shock or the external pressure on the measurement results is not detected.

1. The experiments were performed in a vacuum wind tunnel, for which the diagram of the working section is shown in Fig. 1a. The gas goes through the leak 1 to the mixing chamber 2 equipped with a labyrinth type resistance heater and closed by a cooled screen, then escapes through the cooled nozzle 3 in the strong underexpansion mode into the working chamber where the cooled model 5 is mounted on the plotting board 4

Moscow. Translated from Zhurnal Prikladnoi Mekhaniki i Tekhnicheskoi Fiziki, No. 3, pp. 90-98, May-June, 1982. Original article submitted March 23, 1981.

0021-8944/82/2303-0392 $07.50

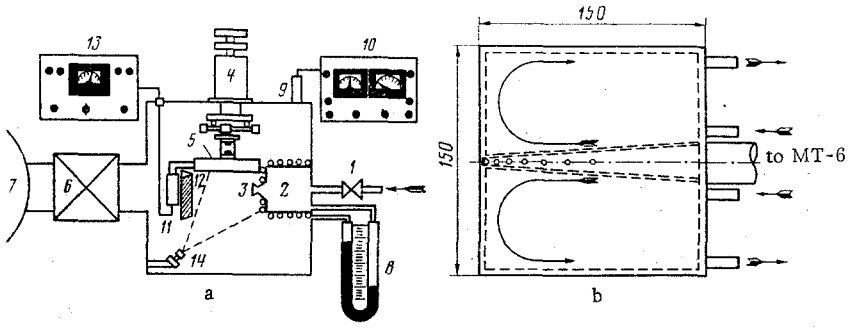

Fig. 1

by using a holder. The working chamber is connected to the buffer capacity 7 through a vacuum seal 6, and the gas is then evacuated by a system of booster and roughing pumps.

The nozzle wall temperature was varied in a number of experiments, and the nozzle was covered by a special cooling shield, a mask, to screen out the radiant heat flux from the nozzle to the model.

The pressure p_0 in the mixing chamber was measured by a U-shaped mercury manometer 8, the pressure in the working chamber p_∞ by the calibrated lamp PMT-2 with the converter VIT-1A (positions 9 and 10, respectively). The gas temperature in the mixing chamber (the stagnation jet temperature T_0) was determined from readings of the calibrated Chromel–Copel thermocouple, whose hot junction was in front of the nozzle entrance on its axis. Research was performed with six nozzles: $M_a = 1$, 1.675, 2.30, 2.88, 3.31, 3.92. The critical diameter fluctuated between $1.5 \cdot 10^{-3}$ and $1.65 \cdot 10^{-3}$ m in the series of nozzles. The exit section of all the supersonic nozzles was conical with a 10° half-angle. Each nozzle is provided with an annular cooling jacket, arranged around the entrance section, but because of the relatively moderate nozzle size and the high heat conductivity of the material effective cooling of the nozzle as a whole was assured, as well as of the vacuum seal (rubber or fluoroplastic) used to maintain the necessary seal at the nozzle-heater connection. Moreover, each nozzle has a special adjusting ring for mutual adjustment of the nozzle, the coordinate mechanism and the model.

The model of the cooled flat obstacle is a square copper housing with the dimensions $1.5 \cdot 10^{-1} \times 1.5 \cdot 10^{-1}$ m^2 covered on the stream side by a thin layer of low-heat-conducting material. The coating is provided with a set of microthermocouple transducers to measure the thermal fluxes to the obstacle by the method of an auxiliary wall [9], whose values were used to estimate the accuracy of the pressure measurement results. The model housing has three cavities: a center measuring cavity to sample the pressure p_w on the obstacle surface, and two lateral cavities with inputs for thermostatic control of the fluid (Fig. 1b). Above the central cavity, the model wall is drained along the axial line by several orifices with diameters $0.55 \cdot 10^{-3}$ and $0.8 \cdot 10^{-3}$ m, only one of which was used in each specific measurement, while the rest were plugged. The relative length of the drainage channel was 1.7-3.8 for different models and different orifices. The measuring cavity is connected to the calibrated manometer sensor MT-6, shielded from the thermal action of the jet by a cooling screen (positions 12 and 11 in Fig. 1a, respectively) by a copper connector. The length of the connecting pipe is $1.7 \cdot 10^{-1}$ m for a mean diameter of about $1 \cdot 10^{-2}$ m. An instrument analogous to a VSB-1 vacuum-gauge (position 13 in Fig. 1a) converts the signal from the MT-6. Distilled water delivered from a thermostat at room temperature cools the screens, the mask, the nozzle and the model. After the model has been set up in the working chamber on the coordinate plotting board, and the model and nozzle have been adjusted relative to its directrix, the model surface and the nozzle axis were out of parallel by not more than 3', which permitted bypassing a comparatively moderate number of drainage holes (usually three-four) to obtain the pressure distribution on the obstacle because of using longitudinal and transverse model displacements. The coordinates of the maximum p_w on the obstacle were determined here simultaneously with high accuracy (0.1-0.2 mm).

The model mounted in the chamber before the beginning of the set of measurements was kept under vacuum for 4-5 days. Then in order to estimate the influence of conductivity and degassing, the model was calibrated, which showed that the difference in the times of pressure equilibration in the working chamber and in the center cavity of the model was not more than 1 min, as is later taken into account in the measurements.

The influence of thermal transpiration in the measuring cavity of the model and the pipeline on the pressure measurement was excluded in advance because the model housing and the whole measuring mainline, including the MT-6 housing, were at the identical temperature, equal to the temperature of the thermostat fluid.

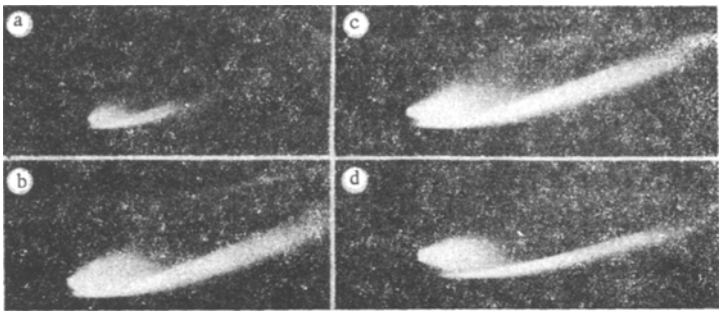

Fig. 2

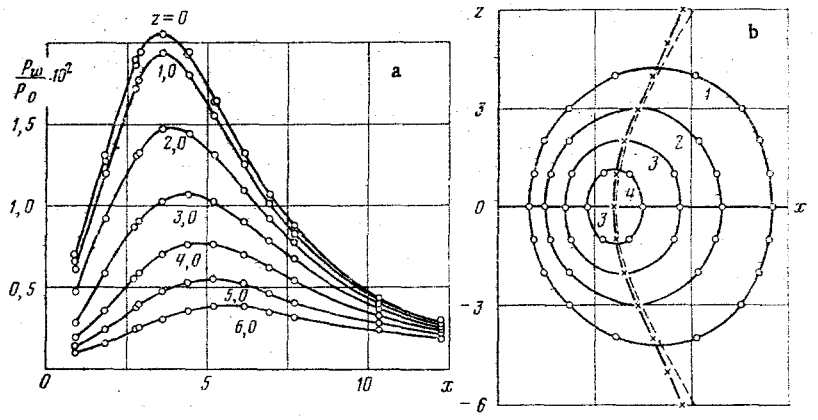

Fig. 3

The influence of thermomolecular effects on the pressure measurement results was estimated by the method in [10]. Computations showed that in the most unfavorable case ($M_a = 2.88$, $T_0 = 780°K$, $p_0 = 4.13 \cdot 10^4$ Pa) the magnitudes of the corrections do not exceed 4.5%. They are around 1% and less in all the remaining regimes, which permitted giving up through correction of the results.

In order to study the geometry of the flow wave structure, it was visualized in the plane of symmetry (the plane passing through the nozzle axis perpendicularly to the obstacle surface). A scanning electron beam produced by an electronic gas discharge gun 14 (see Fig. 1a) was used for this [11]. The electron energy in the beam was 10 keV.

2. Examples of the flow wave patterns above the obstacle are presented for certain cases in the plane mentioned in Fig. 2 for h = 4: a) $M_a = 1.675$, $N = 1 \cdot 10^4$, $Re_* = 7430$; b) $M_a = 2.88$, $N = 2.30 \cdot 10^4$, $Re_* = 7810$; c) $M_a = 3.31$, $N = 1.7 \cdot 10^4$, $Re_* = 7750$; d) $M_a = 3.92$, $N = 1.1 \cdot 10^4$, $Re_* = 7990$.

The shock above the obstacle is curved in both the longitudinal and transverse directions, the perturbed flow behind it is substantially three-dimensional, and the pressure distribution above the obstacle surface should have a peak. A typical view of such a distribution is shown in Fig. 3a for the regime characterized by the following parameters: $M_a = 1$, h = 4, $p_0 = 5 \cdot 10^4$ Pa, $T_0 = 535°K$, $N = 1.61 \cdot 10^4$–$2.95 \cdot 10^4$, $Re_* = 5340$, where $x = X/r_a$, $z = Z/r_a$ are dimensionless Cartesian coordinates of points of the plane passing through the surface of the obstacle. The measurement of x is from the plane of the nozzle exit. The value of the coordinate of the absolute maximum pressure of the obstacle x_m with respect to the "local" focus of the jet, i.e., the quantity $x_m - f$, where $f = F/r_a$ (F is the abscissa of the projection of the jet focus on the obstacle), is predicted fairly by (6) from [5] for the case presented

$$x_m - f = 0{,}5h\sqrt{I_1/(1 - I_1)}. \qquad (2.1)$$

However, for greater h a more forward location of the maximum p_W was obtained for $M_a = 1$ in experiments on low-density jets as compared with the computation by (2.1). The downstream shift of the maximums of the longitudinal side distributions p_W as z increases also deviates gradually from the hyperboloid dependence recommended by the authors [4, 5] (the dashes in Fig. 3b), and actually proceeds more slowly and, moreover, practically linearly for $z \gtrsim 3$. The shape of the isobars for the p_W/p_0 distribution, represented in Fig. 3a, is

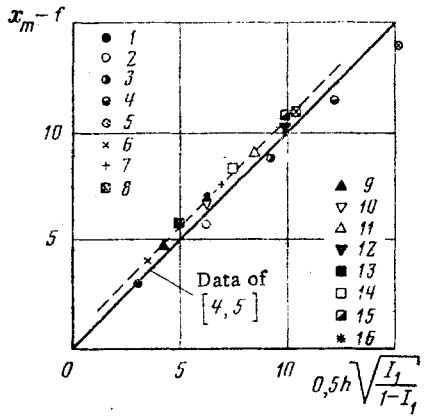

Fig. 4

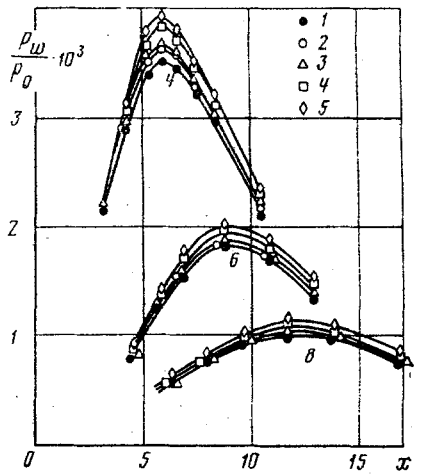

Fig. 5

shown in Fig. 3b: 1) $p_w/p_0 \cdot 10^2 = 0.70$; 2) 1.07; 3) 1.475; 4) 1.90. All the isobars near the maximum $p_w = p_{wm}$ are compressed along the x axis, from which there follows that in this neighborhood $-(\partial^2 p_w/p_0)/\partial x^2 > -(\partial^2 p_w/p_0)/\partial z^2$.

An approximate analysis of the pressure distribution [12] based on the Newton method and the Roberts formula for the density field of a free jet yields an analogous result.

A comparison of the data for measuring the coordinate x_m and the computation using (2.1) is presented in Fig. 4 for different numbers $M_a = 1$, $Re_* = 5340$, h = 4, 8, 12, 16, 20, respectively; 6-8) $M_a = 1.675$, $Re_* = 5390$, h = 4, 8, 12, respectively; 9-12) $M_a = 2.30$, $Re_* = 3020$-6820, h = 4, 6, 8, 9, 35, respectively; 13-15) $M_a = 2.88$, $Re_* = 2800$-6300, h = 4, 6, 8, respectively; 16) $M_a = 3.92$, $Re_* = 8440$, h = 4. In contrast to $M_a = 1$, the measured values of x_m for a low-density jet systematically exceed the computed values for $M_a = 1.675$, but are subject to a linear dependence as are these latter. Experiments showed that x_m is independent of Re_* in the range $Re_* = 2.8 \cdot 10^{-3}$-$8.4 \cdot 10^3$.

However, a change in the number Re_* is reflected by the magnitude of the induced pressure: The pressure on the obstacle decreases somewhat in the neighborhood of the maximum as Re_* diminishes, as is shown in Fig. 5 for $M_a = 2.88$: 1) $Re_* = 2820$; 2) 3150; 3) 3470; 4) 4840; 5) 6250. The change in Re_* was achieved by varying the parameters p_0 and T_0.

All the information presented refers to jets escaping from nozzles with cooled walls, whose temperature T_c equals the model housing temperature T_m. In order to clarify the influence of the thermal nozzle regime on the force loads comparative measurements of the distribution p_w were made for several M_a and fixed Re_* numbers for different values of the nozzle wall temperature factor $t_c = T_c/T_0$: $T_m/T_0 \leqslant t_c \leqslant 1$. It was hence established that the pressure distribution on the obstacle is not responsive to a change in t_c.

3. The criterial representation of the measurement data for the induced pressure distribution on the obstacle along the abscissa axis is presented in Fig. 6a for the recommendations of [4, 5], where $\xi = (x - f) \cdot (x_m - f)^{-1}$, $\eta = (p_w/p_a)h^2/(1 + \varkappa M_a^2)(1 - I_1)$, p_a is the pressure of the nozzle exit computed according to the number M_a. Results of processing experiments on dense jets ($Re_L \sim 10^4$, $Re_* \sim 10^6$) from [12] are shown there (points 1-3), as are also data of tests from [4, 5] (the symbol 4) obtained under analogous conditions, and the curve proposed in [5] for the approximation of the experimental points. The remaining clarification is contained in Table 1.

The point spread relative to the curve mentioned is actually much greater than in [4, 5]. It reaches −20%-+60% in the neighborhood of the maximum.

So great a discrepancy cannot be the result of the influence of the number Re_* or a consequence of processing the measurement data for a low-density jet without taking account of the boundary layer on the nozzle walls. A diminution of Re_* should result in a reduction in the value of η (see Fig. 5); however, a major portion of the array of points in Fig. 6a, displaying the results of tests on low-density jets, is noticeably above the curve in the area of the maximum, and on the other hand, the substantial deviation downward is characteristic for points corresponding to the case of leakage of a dense jet (points 1) when the influence of the num-

TABLE 1

Point number in Fig. 6a and b	M_a	h	Re_*	Point number in Fig. 6a and b	M_a	h	Re_*
1	2	1,98	$\geqslant 8 \cdot 10^5$	*14*	2,88	4	6250
2	2	3,96	$\geqslant 8 \cdot 10^5$	*15*	2,88	4	4840
3	2	6,05	$\geqslant 8 \cdot 10^5$	*16*	2,88	4	2820
4	1,0—3,01	1,97—3,96	$\geqslant 8 \cdot 10^5$	*17*	2,88	6	6250
5	1	4	11500	*18*	2,88	6	4800
6	1	12	11340	*19*	2,88	6	2810
7	1	4	5340	*20*	2,88	8	6300
8	1	8	5340	*21*	2,88	8	4820
9	1	12	5340	*22*	2,88	8	2820
10	1	16	5340	*23*	3,14	4	8700
11	1	20	5340	*24*	3,14	4	6000
12	2,30	4	6820	*25*	3,14	4	4990
13	2,30	8	6820	*26*	3,92	4	8440

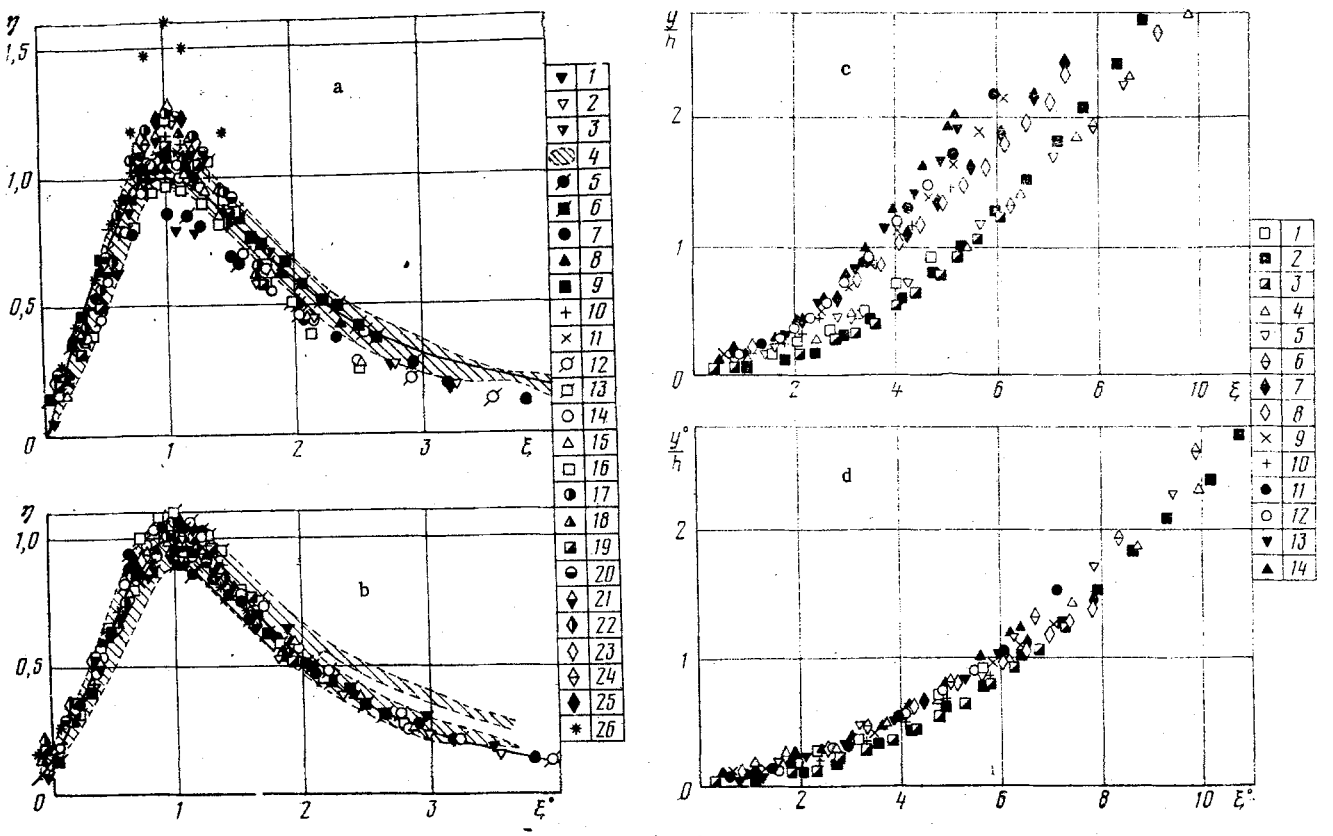

Fig. 6

ber Re_* and the boundary layer on the nozzle walls is insignificant. On the other hand, introduction of the real nozzle number M and the dimensionless distance between the jet axis and the obstacle in terms of effective exit section radii into the computations (by using dependences from [13, 14], say) yields a sufficiently small (to 5%) correction to the value of η in the Re_* range investigated, which is most often also of increasing divergence. Processing the results is here complicated unjustifiedly.

Reasons for the discrepancies between the results in this paper and in [4, 5] are apparently the following.

Fristly, a batch of data quite bounded in the parameter h ($1.6 \leq h \lesssim 4$) is taken in [4, 5] for the extension, while the results of the investigation represented are significantly outside this framework, encompassing even a large range of M_a values as well.

TABLE 2

Point number in Fig. 6c and d	M_a	h	Re_*	Point number in Fig. 6c and d	M_a	h	Re_*
1	3	1,51	$\geqslant 8\cdot10^5$	*8*	1,675	6	7430
2	3	1,60	$\geqslant 8\cdot10^5$	*9*	2,30	4	7040
3	3	2,40	$\geqslant 8\cdot10^5$	*10*	2,30	6	7040
4	2,35	1,51	$\geqslant 8\cdot10^5$	*11*	2,88	4	7810
5	1,94	1,48	$\geqslant 8\cdot10^5$	*12*	2,88	6	7810
6	1,64	1,43	$\geqslant 8\cdot10^5$	*13*	3,31	4	7750
7	1,675	4	7430	*14*	3,92	4	7990

Secondly, utilization of the law of p_{wm}/p_0 variation with respect to h in the form $p_{wm}/p_0 \sim h^{-2}$ for forming the similarity parameter η in the above-mentioned range of h is not completely correct since this law is asymptotic in nature and, therefore, satisfied for large h [3]. For small and medium h an approximation of the form $p_{wm}/p_0 \sim (h^2 + ah + b)^{-1}$, where $a > 0$, $b > 0$, is more justified. It hence follows that the product $(p_{wm}/p_0)h^2$ grows monotonically as h increases (tending to a certain constant value), which agrees with the experiments in this paper and in [2], as well as with the results of computations by the Newton method.

Thirdly, as follows from Fig. 6a, the parameter η does not remain unchanged as M_a changes (but with $\xi \sim 1$, h, Re_* conserved). A monotonically increasing functional dependence is actually traced between them.

Let us note that use of the ratio p_w/p_a is undesirable since the pressure at the nozzle exit is not usually measured. It is more convenient to operate with the quantity p_w/p_0 in practical applications.

On the basis of the ideas in [4, 5], the authors tried to give a new criterial representation of a force load on an obstacle in order to refine the influence of h and M_a and to take account of the number Re_*. The following similarity variables are constructed from the processing results and analysis of experiments for an air jet ($\varkappa = 1, 4$):

$$\eta^0 = \frac{p_w}{p_0}(h^2 + 1.3h + 0.2)\left(1 + \frac{20}{\sqrt{Re_*}}\right)\Big/9(1 - I_1)^{2.26},\quad \xi^0 = 1 + (\xi - 1)\frac{I_1}{I_{11}}.$$

Here I_{11} is the value of I_1 for $M_a = 1$.

Going over to the parameters ξ^0, η^0 results in a diminution of up to $\pm 10\%$ in the scatter of data near the coordinate $\xi^0 = 1$ in the range $M_a = 1$-3.92, h = 1.98-20, and $Re_* \geq 2800$ (see Fig. 6b, where the points are the same as in Fig. 6a). The points in Fig. 6b are approximated satisfactorily by the dependence

$$\eta^0 = [5.28(\xi^0 + 0.41)^2/(5.80 + (\xi^0 + 0.41)^{4.5})].$$

It must be stated that a gradual deviation of a certain part of the results in [4, 5] from the results in this paper and in [2] occurs for $\xi^0 \geqslant 2$ in the new variables, which it is not possible to explain since the formation and conditions for performing the experiments are not presented in [4, 5].

The shock front configuration above the plane in the plane of symmetry of the flow pattern (the plane of visualization) from the results of processing the photographs (see Fig. 2a-d) is represented for $Re_* \approx$ const in the variable of [5] in Fig. 6c, where the coordinate $y = Y/r_a$ is measured along the normal from the plate surface in the visualization plane. Presented here are data on the shock shape from [5], obtained by shadowgraphs on dense jets (points 1-6). A comparison shows that upon interaction of a low-density jet with an obstacle, the compression shock is substantially forced back from its surface, especially at its periphery, by a thick boundary layer. Moreover, within the family of points by which the compression shock profiles above the obstacle are represented for a low-density flow, stratification by M_a number is observed. As is seen from Fig. 6d, satisfactory generalization of all groups of data into a single dependence is achieved by introduction of the variables $y^0/h = (y/h)[1 - 35/(Re_*)^{1/2}]$ and ξ^0. Explanations of Fig. 6c and d are given in Table 2.

The results presented in this paper for an experimental investigation of the "side" effect of a strongly underexpanded jet on a plane obstacle permit refinement of the criterial dependences governing the shock shape above the obstacle and the induced pressure distribution on its surface, and exhibit the possibility of their application in both the case of a jet with a turbulent mixing layer and in the case of purely laminar jets.

LITERATURE CITED

1. E. T. Piesik, R. R. Koppang, and D. J. Simkin, "Rocket-exhaust impingement on a flat plate at high vacuum," J. Spacecr. Rockets, 3, No. 11 (1966).
2. V. A. Zhokhov, "Analysis of the pressure distribution in supersonic freely expanding gas jet flow around a flat plate," Uch. Zap. TsAGI, 4, No. 4 (1973).
3. E. A. Leites, "Flow investigation in the domain of two and four jet interactions," Tr. TsAGI, No. 1575 (1974).
4. E. A. Leites, "Modeling of the strong action of a strongly underexpanded jet on a flat surface parallel to its axis," Uch. Zap. TsAGI, 6, No. 1 (1975).
5. Yu. N. Kononov and E. A. Leites, "Flow parameters in composite jets," Tr. TsAGI, No. 1721 (1975).
6. I. N. Murzinov, "Similarity parameters for the exhaust of strongly underexpanded jets in a submerged space," Izv. Akad. Nauk SSSR, Mekh. Zhidk. Gaza, No. 4 (1971).
7. V. V. Volchkov, A. V. Ivanov, et al., "Low density jets behind a sonic nozzle for large pressure drops," Zh. Prikl. Mekh. Tekh. Fiz., No. 2 (1973).
8. N. I. Kislyakov, A. K. Rebrov, and R. G. Sharafutdinov, "On the structure of high-head low-density jets behind a supersonic nozzle," Zh. Prikl. Mekh. Tekh. Fiz., No. 2 (1975).
9. V. K. Aslanyan, É. N. Voznesenskii, and V. I. Nemchenko, "Features in application of the auxiliary wall method to measure strongly inhomogeneous local heat flux distributions," Inzh.-Fiz. Zh., 35, No. 1 (1978).
10. J. L. Potter, M. Kinslow, and D. E. Boylan, "An influence of the orifice on measured pressures in rarefied flow," Rarefied Gas Dynamics, 4th Symp., Vol. II, Academic Press, New York (1966).
11. V. I. Nemchenko, "Models of compact electron guns for gasdynamic investigations at low pressures," Fourth All-Union Conf. on Rarefied Gas Dynamics. Collection of Abstracts [in Russian], Moscow (1975).
12. A. A. Vasil'ev, V. A. Elizarov, P. G. Itin, and R. M. Kopyatkevich, "Study of the thermal effect of a strongly underexpanded gas jet on a flat surface," Tr. Fourth All-Union Conf. on Rarefied Gas Dynamics and Molecular Gas Dynamics [in Russian], Izd. TsAGI, Moscow (1977).
13. N. I. Yushchenkova, S. A. Lyzhnikova, and V. I. Nemchenko, "On the question of the structure of supersonic gas jets and low-temperature plasmas," Transport Phenomena in a Low-Temperature Plasma [in Russian], Nauka i Tekhnika, Minsk (1969).
14. V. I. Nemchenko, "Influence of the temperature factor on the mass flow factor of a conical supersonic nozzle and determination of the stagnation gas or plasma temperature by the local speed of sound at low Reynolds numbers," Fourth All-Union Conf. on Rarefied Gasdynamics. Coll. Abstracts [in Russian], Moscow (1975).

DEVELOPMENT OF SMALL PERTURBATIONS IN A SLIGHTLY NONPARALLEL SUPERSONIC FLOW

S. A. Gaponov, A. D. Kosinov, A. A. Maslov, and I. V. Semenov

UDC 532.526

Presently the linear theory of stability of plane-parallel flows of a compressible fluid has been rather well developed [1]. Flows encountered in practice are nonuniform in space as a rule. Often one can assume this nonuniformity to be weak (for example, the flow in a boundary layer). In recent years several alternatives have been developed for the construction of a solution when the average parameters of the flow vary weakly in some directions. The first theoretical results for a boundary layer of incompressible fluid which take account of nonparallelness of the flow were obtained in [2, 3]. An experimental check of the conclusions obtained in those papers was performed in [4]. The development of perturbations in a supersonic boundary layer with nonparallelness taken into account was discussed theoretically in [5-7]. Two-dimensional perturbations were treated in [5], and perturbations of a more general kind were treated in [6, 7]. These papers give significantly different results for the very same conditions. Thus, a strong effect of nonparallelness on the stability characteristics is obtained in [6], but a weak effect is obtained in [5, 7]. There are no experimental papers formulated

Novosibirsk. Translated from Zhurnal Prikladnoi Mekhaniki i Tekhnicheskoi Fiziki, No. 3, pp. 98-102, May-June, 1982. Original article submitted April 16, 1981.

0021-8944/82/2303-0398$07.50